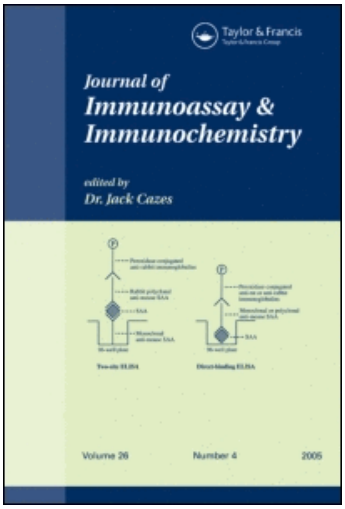

Journal of Immunoassay and Immunochemistry

Publication details, including instructions for authors and subscription information:
http://www.informaworld.com/smpp/title~content=t713597271

A Descriptive Model for the Kinetics of a Homogeneous Fluorometric Immunoassay

Emmanuel Zuber[a]; Laurent Rosso[a]; Bruno Darbouret[b]; Françoise Socquet[b]; Gérard Mathis[b]; Jean-Pierre Flandrois[a]

[a] Laboratoire de bactèriologie, CNRS UMR 5558, Faculté de médecine Lyon Sud, France [b] Division In Vitro Technologies, CIS Bio International, France

To cite this Article Zuber, Emmanuel , Rosso, Laurent , Darbouret, Bruno , Socquet, Françoise , Mathis, Gérard and Flandrois, Jean-Pierre(1997) 'A Descriptive Model for the Kinetics of a Homogeneous Fluorometric Immunoassay', Journal of Immunoassay and Immunochemistry, 18: 1, 21 — 47

To link to this Article: DOI: 10.1080/01971529708005803

URL: http://dx.doi.org/10.1080/01971529708005803

JOURNAL OF IMMUNOASSAY, 18(1), 21–47 (1997)

A DESCRIPTIVE MODEL FOR THE KINETICS OF A HOMOGENEOUS FLUOROMETRIC IMMUNOASSAY

Emmanuel Zuber[1], Laurent Rosso[1],
Bruno Darbouret[2], Françoise Socquet[2], Gérard Mathis[2],
and Jean-Pierre Flandrois[1]

[1] Laboratoire de bactériologie, CNRS UMR 5558,
Faculté de médecine Lyon Sud, BP 12, Oullins Cedex, France.

[2] Division In Vitro Technologies, CIS Bio International,
BP 175, 30203 Bagnols-sur-Cèze Cedex 05, France.

ABSTRACT

A descriptive mathematical model was chosen to fit the antigen-antibody association kinetics of a new homogeneous immunometric assay for prolactin, involving time-resolved fluorescence detection (TRACE® technology, Time Resolved Amplified Cryptate Emission). We paid special attention to the methodology and criteria applied, to yield a convenient and statistically valid model, designed to allow potential exploitation of kinetic information in the data processing of the assay. We compared specific parameterizations of an hyperbolic model, the Gompertz, and the monomolecular models on the basis of morphological considerations, a statistical analysis of fit, and an assessment of the parameters estimation quality, over a wide range of antigen concentrations. The monomolecular model gave the best fit, and the most precise and stable estimation of its parameters. The study of parameter properties confirmed this choice.

(KEY WORDS: mathematical modelling, antigen-antibody reaction, time-resolved fluorometry)

INTRODUCTION

Mathematical modelling of antigen-antibody reactions has been widely used in an attempt to formalize the interactions between different molecular species by means of classical chemistry laws (mechanistic approach) (1, 2, 3, 4). However, since the introduction of the radioimmunoassay, the use of these very specific reactions for a variety of commercial, medical and scientific purposes has led to the automation of such assays and of their data processing. This trend has fostered the use of mathematical modelling in a descriptive rather than mechanistic approach, in order to obtain reliable assay results in the most convenient and precise manner (1, 5, 6, 7). Indeed, mechanistic models are generally not suitable for this kind of application, mainly because of their great number of parameters, which are often poorly identifiable from the data and without any convenient graphical meaning (5, 8). These disadvantages may be circumvented by the formulation of an appropriate descriptive model, the claim of which would merely be to account for the observations.

We describe the choice of such a descriptive model, to fit the kinetics of a new homogeneous liquid phase fluorometric immunoassay for prolactin. Thanks to the TRACE® technology (Time Resolved Amplified Cryptate Emission), this assay allows the kinetics of the antigen-antibody complex formation to be directly followed with a good sampling frequency (in our case: one point every 120 seconds), without interfering in the reaction process. This innovating feature is likely to offer not only valuable insights into the actual chemical mechanisms underlying the system (which is beyond the scope of this

study), but also a new source of information for the development of a more efficient data reduction package for routine analysis. Several authors have reported interest in the use of kinetic data in a general immunoassay data processing approach (9, 10), but such attempts have remained limited because of technical difficulties in obtaining these data (11).

The purpose of this study was to obtain a model with properties of convenience and statistical quality suitable for a precise, stable and, if possible, early estimation of the curve characteristics. This is the first step in a broader study scheme aimed at the eventual exploitation of kinetic information in the assay data reduction system. At this stage, special care has been taken in the application of a methodology and a set of criteria for constructing and assessing models from a general evaluation of their behavior. This ensured the suitability of the chosen model for kinetics description over a wide range of analyte concentrations, and pinpointed the experimental domain which should be further investigated. The proposed proceedings may apply in any descriptive modelling approach, where the emphasis is on the estimation quality of the parameters rather than on their theoretical significance.

MATERIALS AND METHODS

Reagents and Procedures

Assay

This work was performed on a two-site immunometric assay of

prolactin (12, 13), a 23 kDa peptide hormone (Calbiochem AG, Luzern, Switzerland), considered here as a model case for kinetic analysis. This homogeneous liquid phase assay was based on the time-resolved fluorometric detection of the energy transfer between two different labels, each on a specific antibody (12) (TRACE® technology, Time Resolved Amplified Cryptate Emission). According to this methodology principle, one of the antibodies was labelled with the donor, an europium(III) cryptate (CIS Bio International, Bagnols/Cèze, France), and acceptor molecules (XL 665, a chemically modified allophycocyanine, CIS Bio International) were covalently bound to the second antibody. When both antibodies were involved in an immune complex, the donor transfered part of its laser excitation energy to the acceptor. XL 665's subsequent fluorescent emission was then detected.

Monoclonal antibodies were produced on location by CIS Bio International. Donor and acceptor antibody labelling was performed at CIS Bio International (Bagnols/Cèze, France), as described by Lopez *et al.* (14). Prolactin initial concentrations were expressed in international units per litre (IU/L), quantifying its biological activity.

After addition of 100 µL of antigen solution, the assay medium consisted of a 300 µL solution containing 200 µL of a 100 mmol/L, pH 7 phosphate buffer supplemented in fluoride ions by 600 mmol/L KF (initial concentration) and in Bovine Serum Albumin (BSA, 1%, Interchim, Montluçon, France), and 100 µL of new-born calf serum (Jean Tastet, Cassen, France) to simulate a serum like medium. Final antibody concentrations were $1.1\ 10^{-9}$ $mol.L^{-1}$ for the donor and $1.1\ 10^{-8}$ $mol.L^{-1}$ for the acceptor.

Apparatus

The assay was performed with a prototype of a dedicated apparatus (KRYPTOR®) designed by CIS Bio International and realized by Packard Instruments Company (Camberra Industries, Downers Grove, Il, USA). This allowed the kinetics of several samples to be followed simultaneously in disposable plastic cupules held in a 37°C temperature controlled chamber.

The monochromatic excitation of the donor was done by a nitrogen laser beam. The fluorescence was measured at two different wavelengths through a set of beam-splitters and two photomultipliers connected to a photon counter, according to the time-resolved fluorescence detection principle (12, 15, 16).

Data

The modelled variable was the dimensionless ratio R of the integrated counts over a time lapse of 1 second at 665 nm (acceptor emission wavelength) divided by the same integration of counts at 620 nm (donor emission wavelength). It represented the immune complex specific emission corrected for the optical density of the medium (12, 17). This ratio was then multiplied by 10^4 for representation convenience.

A series of 12 kinetic data sets was used for the comparison of the models. Each data set corresponded to a kinetics with a different antigen concentration, ranging from 0.222 to 9.229 IU/L. The concentrations for each kinetics are detailed in Table 1. All the kinetics

were followed simultaneously for one hour under the same experimental conditions. Sampling rate was one point every 120 seconds, giving a data set of 31 points.

The time 0 data point of kinetics 1 has been deleted because of its excessive, obviously outlying value.

Models

Three descriptive models were considered for the representation of the variation of the fluorescence ratio (R, dimensionless) versus time (t, in seconds). They were chosen for their morphological behavior, corresponding to the apparent shape of experimental data. All of them have three parameters, chosen for their graphical or chemical signification, given that in regression analysis, the least parameters, the better the model (7).

The Monomolecular model (M). A specific parameterization of this classical model (18) has been studied:

$$R(t) = R_m - (R_m - R_o)\ e^{-\left(\frac{S_o}{(R_m - R_o)}\right)t} \qquad [1]$$

with: R_o: ordinate at time t=0 s (dimensionless)

R_m: horizontal asymptote corresponding to maximal R (dimensionless)

S_o: slope at time t=0 (s-1).

The Hyperbolic model (H). Proposed merely from morphological considerations, this model is nevertheless related to a simplified second order kinetic law with negligible dissociation and equal initial concentrations in antigen and antibody, as proposed by Hertl et Odstrchel (3) for heterogeneous reactions:

$$\frac{x}{R_m(R_m - x)} = kt \qquad [2]$$

with: x: bounded antigen fraction (dimensionless)

R_m: horizontal asymptote corresponding to maximal x (dimensionless)

k: apparent kinetic constant (s^{-1})

Parameter k may indeed be expressed as a function of R_m and of the slope at time t=0 (parameter S_o), and a parameter representative of the ordinate at time t=0 (R_o) may be added. After simplification, one gets equation [3].

$$R(t) = Rm - \frac{(Rm - R_o)^2}{S_o t + (Rm - R_o)} \qquad [3]$$

The Gompertz model (G). Its usual parameterization is the following (18):

$$R(t) = R_o e^{\left[\frac{A}{\mu}\left(1-e^{-\mu t}\right)\right]} \qquad [4]$$

with: R_o: ordinate at time t=0 s (dimensionless)

A: slowing factor (s^{-1})

μ: slope factor (s^{-1}).

With R_m denoting the horizontal asymptote (for $t \to \infty$), it is possible to show that:

$$A = \mu \left(\ln(R_m) - \ln(R_o) \right) \qquad [5]$$

Replacing parameter A by equation [5], one gets the following parameterization:

$$R(t) = R_m \left[\frac{R_o}{R_m}\right]^{e^{-\mu t}} \qquad [6]$$

with: R_o: ordinate at time t=0 s (dimensionless)

R_m: horizontal asymptote corresponding to maximal R (dimensionless)

μ: slope factor (s^{-1}).

Data Analysis

The ordinary least squares criterion (noted SSR, standing for "Sum of the Squared Residuals") was used to **fit the model** to the data. The minimum SSR values (SSR_{min}) were computed in double precision with calls to IMSL 1.1 subroutine DUMINF (IMSL Inc., Houston, TX, USA) which is a derivative-free modification of the usual Levenberg-Marquardt algorithm (30). Starting values were graphically estimated for the parameters having a clear graphical meaning. An adequate initial guess for model G's parameter μ was empirically determined.

To check convergence to optimal parameter values ("**convergence validation**") and thereby model robustness, each computation was then repeated with 8 different sets of parameter starting values (2^3, since all the chosen models have three parameters), located symmetrically to the first starting values with respect to the first parameter estimates.

A statistical analysis of the validity of the regression assumptions was performed in order to assess the fit, and global adequacy of the models for kinetics description over the whole studied range of analyte concentration. This included:

- comparisons on the basis of the minimum of the convergence criterion ($\mathbf{SSR_{min}}$ in our case).
- a test on the **normality of the residual** distribution, using Normal Quantiles -Residual Quantiles plots. (19).

- plots of the **residuals versus time**. Their independence was also checked by a classical runs test (19).

Confidence regions (α=0.05) for parameter estimates were defined according to Beale (20) and determined with a previously described program (21), so that the deduced parameter confidence limits would not be as underestimated as with standard approximate marginal confidence limits. **Relative confidence intervals** were calculated from these boundaries by the ratio of the confidence interval amplitude over the corresponding parameter estimate.

The **parameter properties** were then studied for the chosen model by:

- plotting their estimates and confidence limits versus concentration.

- plotting comparatively as a function of time the dose-response curves obtained from the data, and from the estimate of a parameter (S_o) of the chosen model. This was made by truncating the twelve data sets, taking successively the last point off. The last point left in the truncated data set was directly used for the data dose-response curve labelled with its abscissa t_m, and the chosen model was fitted to yield the corresponding estimation of parameter S_o. To fit the model to each new truncated data sets, a heuristic procedure was set up to automatically give new initial parameter estimates from the data. Convergence validation was also performed for every new fit.

RESULTS AND DISCUSSION

Parameterization Analysis

The simulations of each parameter's independent effect on the

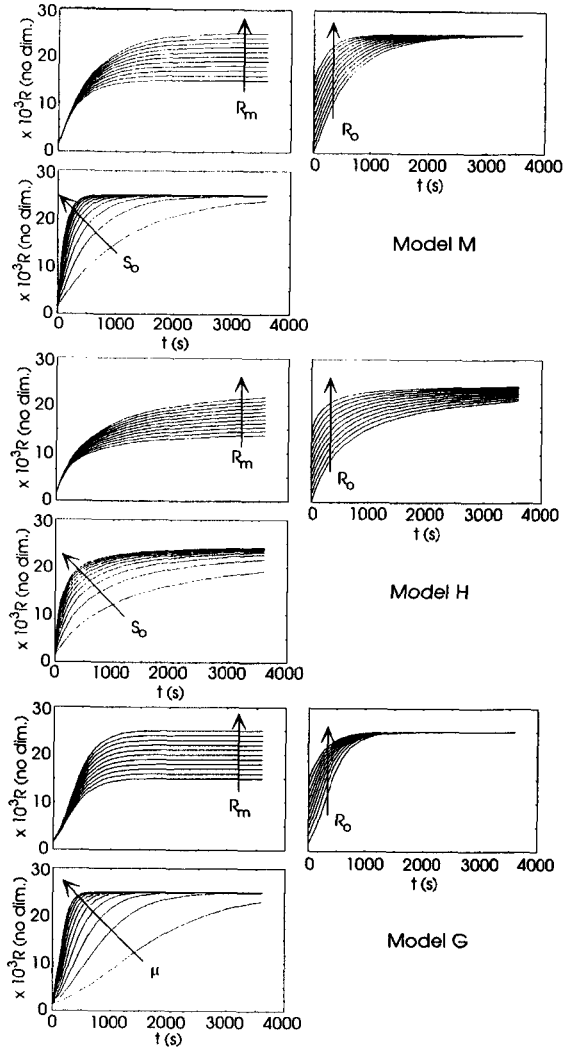

FIGURE 1
Simulations of the effect on the curve shape of each parameter's independent variation, for the three models. R_m varied from 15,000 to 25,000, every 1,000, R_o from 0 to 15,000 every 1,500, S_o from 20 to 200 every 20 and μ from 0.001 to 0.01 every 0.001. When fixed, parameter values were respectively: 25,000 for R_m, 1,400 for R_o, 40 for S_o, and 0.004 for μ.

curve shape (Fig. 1) demonstrated clearly defined influence domains which did not heavily overlap, for each parameter of models M and G. Therefore, no strong structural correlation between the parameters of these models could be expected at this stage of the study. On the contrary, in the given R and t ranges, all three parameters of model H showed an effect on the end of the curve. If sampling was not pursued further in time, a correlation between these parameters might therefore exist for model H when fitting these data.

Statistical Analysis of Fit

Graphics and plots from this analysis were gathered together for each model and each kinetic curve on a record sheet, as shown for kinetics 10 on Figures 2 to 4. Figure 5 also allows the graphical comparison of the three models fit to kinetics 2 data.

Fitting Adequacy

The **convergence validation** never pointed out a failure of SSR minimization for models H and M, even for the fits of the latter on truncated data sets. But it demonstrated erratic SSR_{min} and parameter estimates for kinetics 5 to 10 for model G. A better initial value for parameter μ solved the problem. This was an illustration of the lack of convenience of models having one or more parameters without a clear graphical meaning, these parameters being therefore difficult to initially estimate.

The **visual quality of fit** of model M was satisfactory for all the data sets (Fig. 2 and 5). Model H demonstrated a poor behavior (see Fig. 3

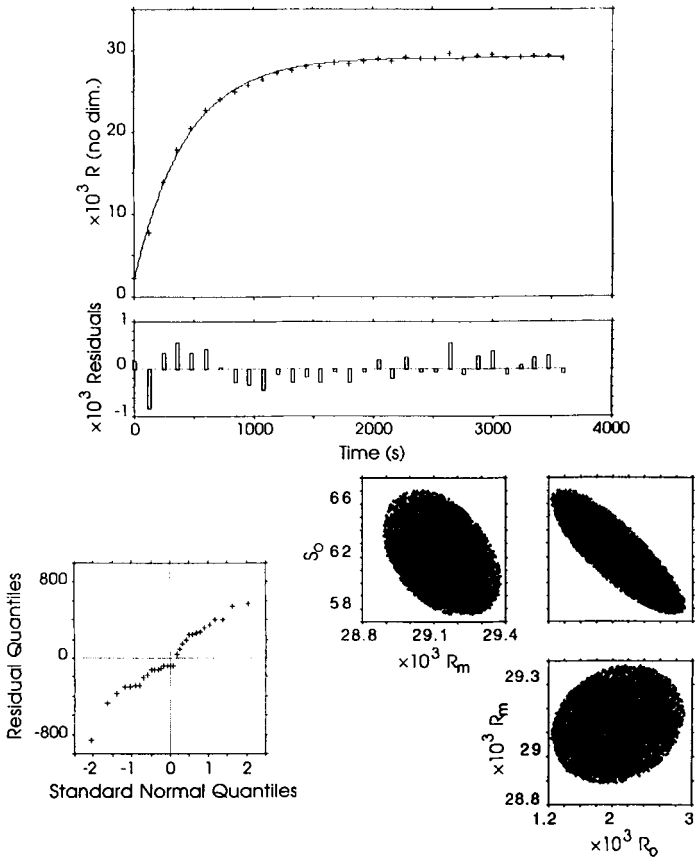

FIGURE 2

Record sheet of the fit of the monomolecular model (**M**) to kinetics 10. **Top chart:** data points with the theoretical curve superimposed, and the plot of residuals versus time. **Middle-right chart:** 95% confidence regions on the parameters. **Middle-left chart:** Normal Quantiles - Residuals Quantiles plot. **Bottom chart:** summary of the convergence results. SSR_{min}: minimum of the sum of the squared residuals; Residual correlation: as tested by the runs test with a level of significance α; Confidence intervals on parameter estimates: these were deduced from the 95% confidence regions.

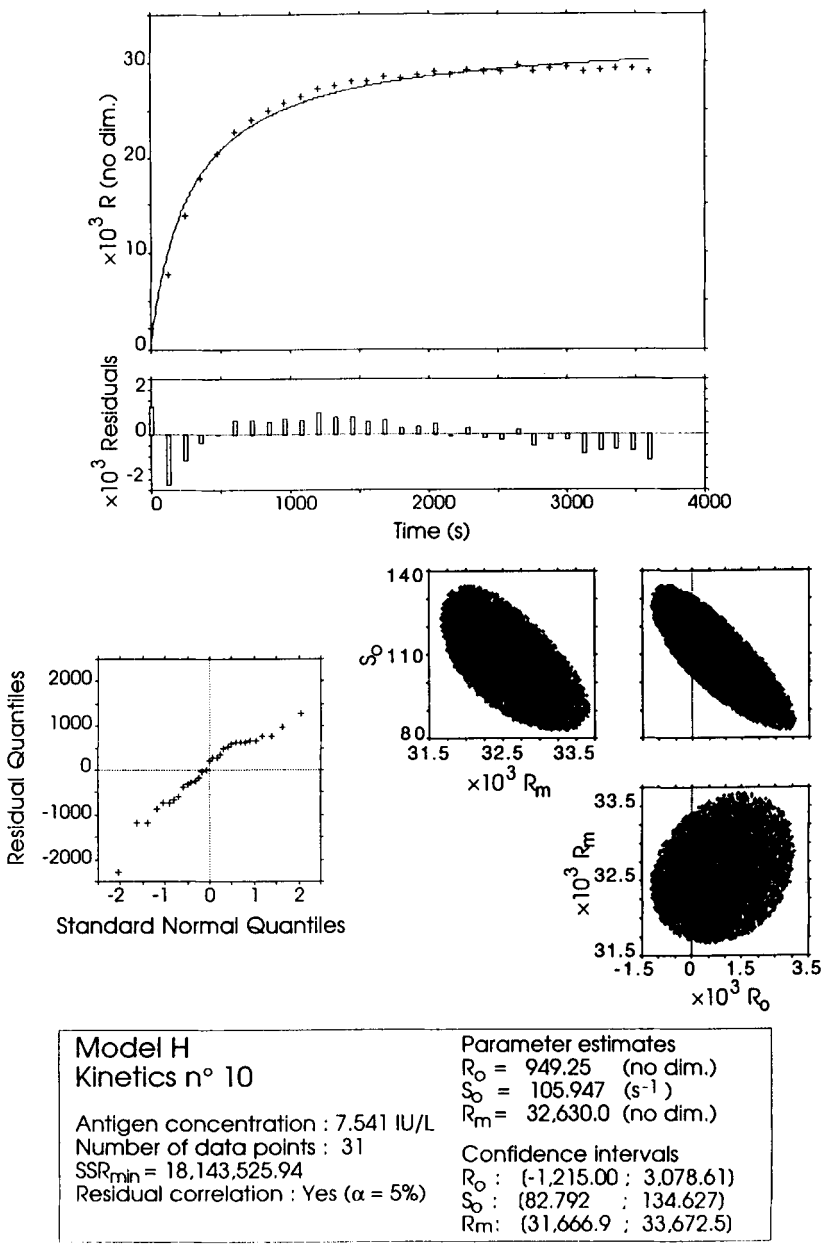

FIGURE 3
Record sheet of the fit of the hyperbolic model (**H**) to kinetics 10. (Item description: see legend of Fig. 2).

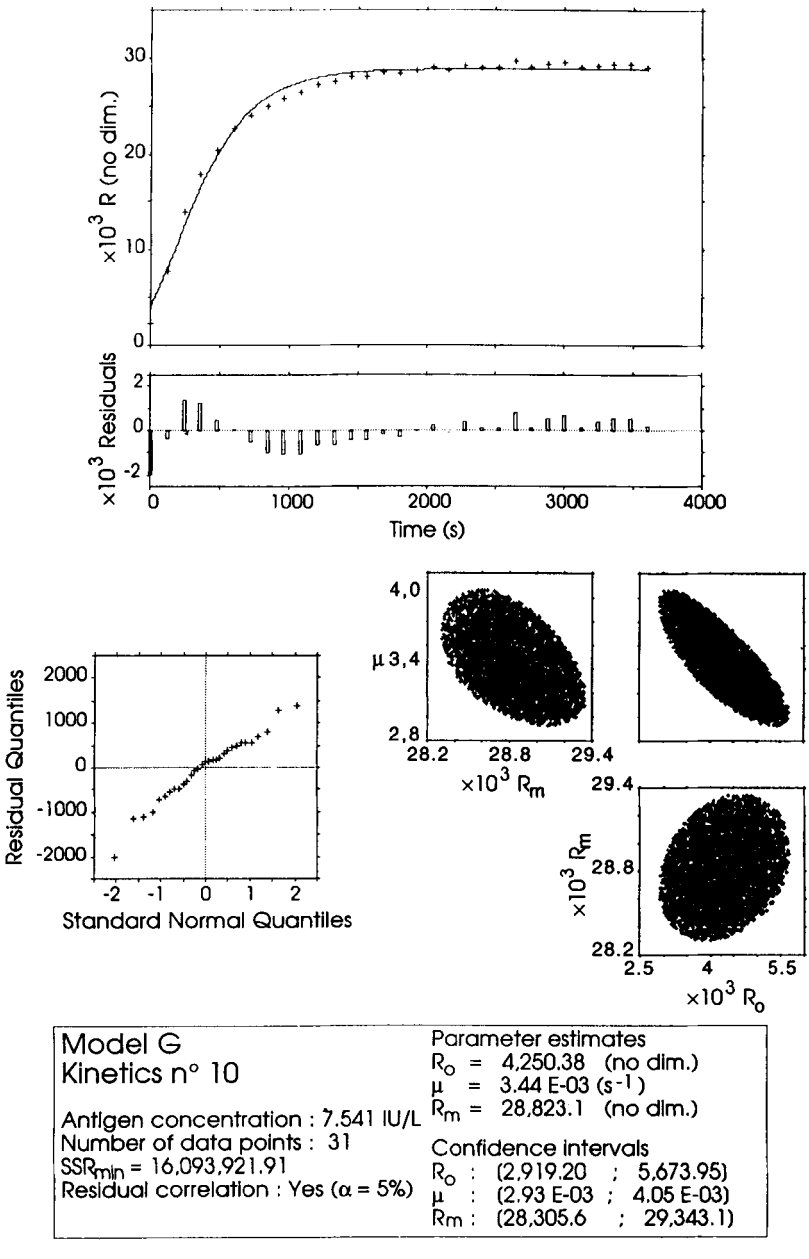

FIGURE 4
Record sheet of the fit of the Gompertz model (**G**) to kinetics 10. (Item description: see legend of Fig. 2).

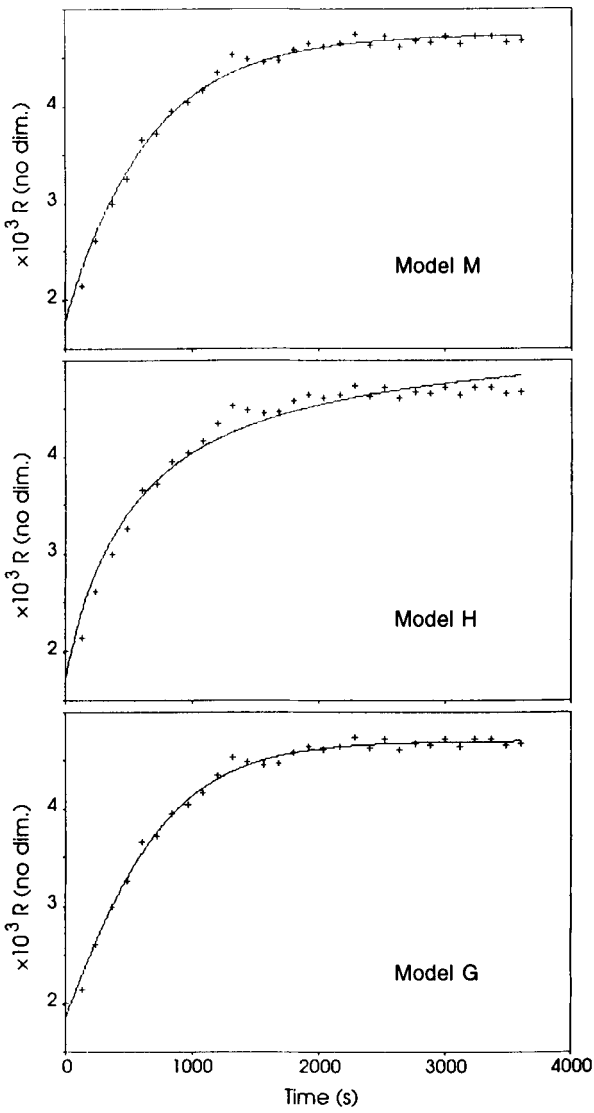

FIGURE 5
Comparative representation of the fit of the three models (**M**: monomolecular model, **H**: hyperbolic model, **G**: Gompertz model) to kinetics 2 (Antigen concentration: 0.468 IU/L). The three theoretical curves were superimposed to the same 31 data points.

TABLE 1

Minima of the Sum of the Squared Residuals ($\mathbf{SSR_{min}}$), and Residual Analysis Results obtained with the three Models (**M**: monomolecular model, **H**: hyperbolic model, **G**: Gompertz model) fitted to twelve kinetics data sets (**curve**).

The smallest SSR_{min} for each data set appears in bold face. **Conc.**: Prolactin initial concentrations. **Res. correl.**: Yes = presence of a residual correlation, as tested by the runs test at the level of significance α=5%. **Outliers**: visual assessment, from the Normal Quantiles - Residual Quantiles plots, of the number of points departing from a normal distribution. ø: obviously non-normal distributions.

kinetics curve N°	Conc. (IU/L)	SSR_{min} ($\times 10^3$) M	H	G	Res. correl./Outliers M	H	G
1	0.222	44	93	**43**	No/0	No/ø	No/0
2	0.468	187	544	**117**	No/3	Yes/2	No/ø
3	0.929	347	1,527	**232**	No/5	Yes/0	No/2
4	1.938	**515**	4,183	813	No/3	Yes/4	Yes/0
5	2.793	**1,136**	8,649	2,002	No/3	Yes/3	No/6
6	3.716	**1,531**	9,539	5,295	No/1	Yes/3	Yes/ø
7	4.491	**1,358**	14,104	5,409	No/2	Yes/1	Yes/3
8	5.462	**3,078**	12,693	11,323	No/1	Yes/1	Yes/ø
9	6.300	**4,904**	11,982	17,469	Yes/2	Yes/1	Yes/1
10	7.541	**3,143**	18,144	16,094	No/1	Yes/ø	Yes/1
11	8.709	**3,785**	22,035	16,542	No/1	Yes/ø	Yes/1
12	9.229	**4,418**	25,254	15,918	No/1	Yes/1	Yes/2

and 5), especially for the first kinetics. Model G fitted the data well for kinetics 1 to 5 (Fig. 5), and then exhibited a consistently bad fit around the bending region of the kinetic curves (e.g. Fig. 4). These results were corroborated by the **comparison of $\mathbf{SSR_{min}}$** values (Table 1). Model H SSR_{min} was indeed always larger than the other model's but for kinetics 9 (Model G's), while model M SSR_{min} was the smallest for the

9 last data sets. The global quality of fit of the models over the whole range of antigen concentration studied could therefore be ranked significantly (Wilcoxon Signed Rank Test, p=0.0096 and p=0.015 respectively) on the basis of the SSR_{min} values: M > G > H. This criterion was equivalent to a direct comparison of the residual variances. The latter indeed had the same degrees of freedom for a given data set, since all the models had the same number of parameters.

Residual Analysis

The regression assumptions stipulate that the residuals should be normally and independently distributed.

The observation of **Normal Quantiles - Residual Quantiles plots** for each kinetics suggested that the distribution was always normal for model M (Table 1), the residual quantiles following a fairly straight line pattern (e.g. Fig.2). Models H and G showed three plots strongly departed from a straight line. The corresponding distributions were therefore considered non-normal (Table 1 and Fig. 3), which suggested that these two models could not be appropriately fitted with the least squares criterion in these cases. The Quantiles - Quantiles plots also allowed the detection of outliers (19), although somewhat subjective. The smallest residual quantile on Figures 2 and 4 gives an example of such a point. It was interesting to note that outliers obtained with models M and H were almost always located at the beginning of the curves (mainly the first and second points). These may either point out questionable data points or regions of lesser adequacy of the

models. In the latter case, a closer look at this region of the kinetics curve, through the use of a higher sampling rate, could help determine whether this phenomenon should be taken into consideration by the model, for example as a very rapid change of concavity (inflexion point) at the beginning of the curve. The actual data sets can not yield sufficient information to allow a correct estimation of such a possible feature of the system by a more complicated model.

The models being strictly monotonous, the plots of the residuals versus time also represent the residuals versus the predicted variable, which may be used to assess the homogeneity of the residual variance along the curve. These plots actually did not allow the detection of any **heteroscedasticity** for models M and H: the amplitude of the residuals did not consistently increase or decrease versus t. This justified the use of ordinary SSR as the convergence criterion in these cases. Observation of the data did not indeed suggest a probable error distribution and no weighing seemed to be necessary, although this was often suggested for immunoassay data in the literature (6, 22, 23). By contrast, a residual variance slightly decreasing in time could be observed for kinetics 6 to 12 fitted with model G (Fig. 4). This could be directly related to the declining quality of fit of this model in the first part of the kinetic curve for increasing concentrations.

These residual plots revealed an **autocorrelation** of the residuals for several kinetics. The residual amplitudes indeed followed non-random wave-like patterns in time (e.g. Fig. 3 and 4). This observation was validated by the runs test results, indicating correlated residuals for 10 kinetics for model H (Table 1), 8 for model G and only a single

data set for model M. This suggested that autocorrelation mainly stemed from the inadequacy of models H and G, rather than from the data, even though an autocorrelation may be expected in high sampling rate time series.

As far as the regression assumptions were concerned, only the fit of model M seemed always justified, but once (see kinetics 9 autocorrelated residuals), using the SSR as the convergence criterion. Both other models showed weaknesses which might lead to a bias in parameter estimation.

Parameter Estimation Precision and Correlations

The shape of the 95% **confidence regions** consistently indicated for the three models, a very slight (quasi-absent for model M) positive structural correlation between parameters R_o and R_m, whereas there was a more pronounced negative correlation between R_o and S_o or μ (e.g. Fig. 2 to 4). The correlation between R_m and S_o or μ was moderate and seemed lighter for model M than for models H and G. The more structurally correlated the parameters, the less stable their estimation from the data set. In the present cases, these correlations never affected the estimation procedure, since neither of the confidence regions appeared non-bounded or severely stretched along one of the diagonals. Thus, the models may not be considered over-parameterized regarding the data (24), which means each parameter estimate corresponds to a specific piece of information from the kinetic data. The correlations appeared to alter the precision on parameter estimates, especially for model H. Some senseless negative

TABLE 2

Relative Precision of Parameters Estimation ($\mathbf{R_o}$: signal at time t=0 s, $\mathbf{R_m}$: maximal signal, $\mathbf{S_o}$: slope of the kinetics curve at time t=0 s, and μ: slope factor) for the three Models (**M**: monomolecular model, **H**: hyperbolic model, **G**: Gompertz model).
Relative Confidence Intervals: Relative amplitude of the 95% confidence interval of each parameter, with respect to its estimated value (as a percentage). The smallest intervals appear in bold face.
a: comparisons between the precision of estimation of parameters μ and S_o are not mathematically justified (see text).

kinetics	Parameter Relative Confidence Intervals (in %)								
curve	R_o			S_o or μ^a			R_m		
number	M	H	G	M	H	G	M	H	G
1	19.60	84.64	**15.37**	**40.69**	137.43	26.93[a]	2.14	5.41	**2.01**
2	19.72	38.95	**13.70**	**30.75**	73.10	19.27[a]	3.11	9.28	**2.25**
3	27.66	70.77	**17.12**	**21.75**	62.74	14.72[a]	2.51	8.76	**1.87**
4	35.50	141.08	**25.89**	**15.15**	59.78	16.48	**1.81**	8.37	2.10
5	53.58	219.41	**35.56**	**16.92**	62.24	19.56	**1.91**	8.29	2.38
6	60.34	257.12	**50.53**	**16.47**	54.96	27.71	**1.85**	7.06	3.24
7	61.11	371.71	**48.77**	**12.80**	57.02	24.13	**1.49**	7.35	2.77
8	82.36	333.09	**64.47**	**18.46**	49.03	33.48	**1.99**	6.12	3.64
9	92.49	308.11	**70.56**	**20.92**	43.25	37.32	**2.30**	5.52	4.12
10	79.83	452.32	**64.81**	**15.18**	48.93	32.72	**1.68**	6.15	3.60
11	90.37	503.63	**68.00**	**16.39**	52.61	32.97	**1.72**	6.20	3.44
12	103.65	552.34	**70.39**	**17.62**	54.91	32.41	**1.77**	6.21	3.21

confidence limits were even observed for R_o with this model (e.g. Fig. 3).

The parameter **relative confidence intervals** (Table 2) always showed a much lower precision of estimation of parameters R_o, R_m and S_o with model H than with the others. Model G allowed the most precise estimation of parameter R_o. Model M gave the best results 9

times over 12 for parameter R_m. Since the two parameters do not have the same mathematical significance, it would be improper to directly compare the precision of estimation of μ (with model G) and of S_o (with models M and H).

On the basis of this analysis, model M seemed to be the most appropriate to account for the data obtained at the different antigen concentrations. Its convenience and quality of fit, the independence and normality of its residual distributions, the precision and low level of correlations of its parameter estimations were overall better than those of models G or H. It was therefore chosen, provided that its parameter properties could allow its use in a data reduction approach.

Parameter Properties

The correlations of parameters S_o and R_m with antigen concentration (Fig. 6) indicated that both parameters could be considered as concentration estimates, though with different properties. Parameter S_o was estimated with a lower precision than R_m, but the relation to concentration of the latter bent to a plateau, corresponding to a saturation of the antigen binding sites.

The correlation between S_o and concentration seemed to be linear, except for the last three points ($r = 0.996$). Though a descriptive model, model M formulation was nevertheless based on a first order kinetic equation. Therefore, the linearity of the S_o-concentration relation corroborated the hypothesis of a pseudo first order mechanism regarding antigen concentration for this antigen-antibody kinetic system. This is consistent with previous observations (2, 25) and with

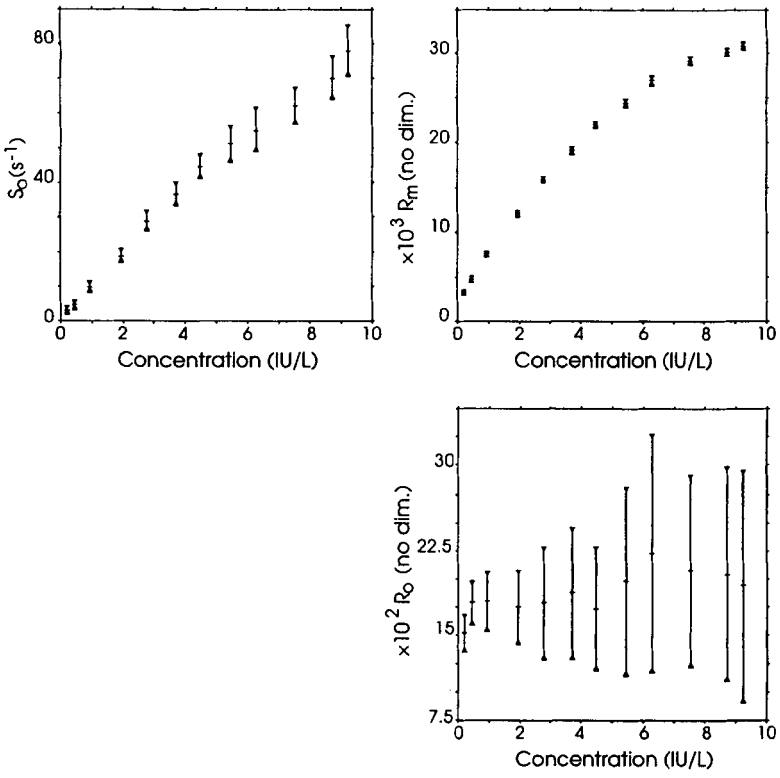

FIGURE 6
Model M parameter (S_o, R_m and R_o) estimates versus prolactin concentration. Triangles indicate the limits of the confidence intervals.

the large antibody excess at low prolactin concentrations. The antigen-antibody concentration ratio dropping down by a factor of 40 between kinetics 1 and 12, departure from this linear relation may be indicative of a change in the system's kinetic behavior, which may require further investigation, for example, at higher antigen concentrations.

According to Figure 7b, this relation between S_o and concentration was very stable regarding the duration of kinetics follow-up, as

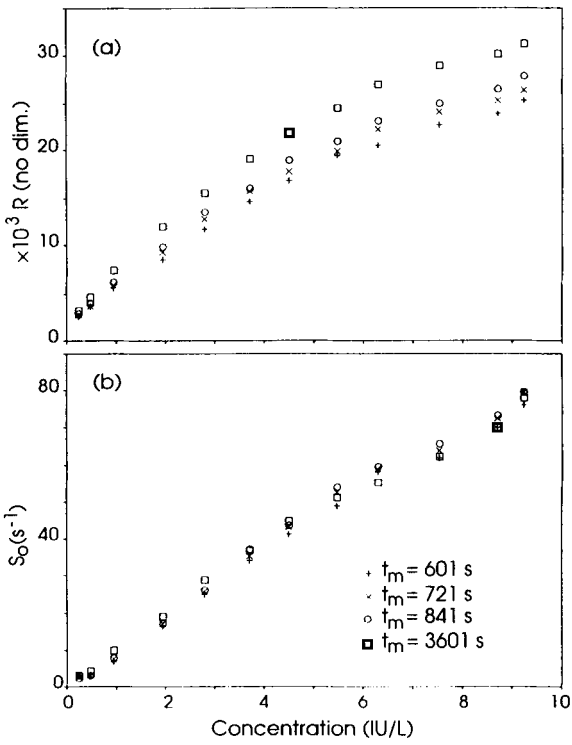

FIGURE 7
Dose response curves obtained at different times by considering the last data point of the data set (a), or the estimated value, from the corresponding data set, of parameter S_0 of the monomolecular model (b). Figure legend applies to both charts (a) and (b), and gives the abscissa t_m (date in s) of the last data point left in the data set.

compared to the last measured data point's dose-response curve, which tended to reach its plateau at ever lower concentrations (Fig. 7a). Even though lacking precision at low dose, the early estimated dose-S_0 relation may therefore show a better ability to discriminate quickly and reliably between high antigen concentrations. It should be noted that at the dates t_m considered here, parameter R_m

could only be estimated by extrapolation, the data sets being truncated before equilibrium was reached. This did not seem to overly affect the estimation accuracy of parameter S_0, thanks to the low level of correlation between both parameters.

Conclusion

Following a general descriptive modelling methodology, we have chosen a model to represent the kinetic data of a new homogeneous fluorometric immunoassay for prolactin. This monomolecular model has better visual and statistical quality of fit, precision of parameter estimations and robustness than the Gompertz, and the hyperbolic model which we also proposed. Moreover, its convenient parameterization allows a rough graphical estimation of the parameter values (e.g. as convergence starting values), and the relations existing between two parameters and concentration suggest their possible incorporation in the assay data reduction software.

This may become of particular interest for parameter S_0. Its extended exploitable dose-response curve towards high concentrations, and good stability of estimation even after short periods of kinetics follow-up, indeed qualify it as a potential early high-concentration estimate. An optimization of the sampling design and a closer study of the first kinetic points could help improve its estimation precision, especially at low dose. Then again, this parameter's properties may also help to investigate the system's kinetic mechanisms and their limits.

In the perspective of an ultimate incorporation of the model parameters in a data reduction package, the next step of this work

should comprise a study of the reproducibility of their properties in a variety of situations, considering for example, between batch variability and real serum sample responses.

ACKNOWLEDGEMENTS

We thank Mrs. Nathalie Giorgis for her technical assistance.

This work was supported in part by a grant from CIS Bio International to E. Zuber.

Corresponding author: E. Zuber, Laboratoire de bactériologie, CNRS UMR 5558, Faculté de médecine Lyon Sud, BP 12, Oullins Cedex, France.

REFERENCES

1. Thakur, A.K. Statistical Methods for Serum Hormone Assays. In: Keel, B.A., Webster S.W., ed. Handbook of the Laboratory Diagnosis and Treatment of Infertility. Boca Raton, FL: CRC Press, 1990: 271-90.

2. Dandliker, W.B. and Levison, S.A. Investigation of Antigen-Antibody Kinetics by Fluorescence Polarization. Immunochemistry 1968; 5: 171-83.

3. Hertl, W. and Odstrchel, G. Kinetic and Thermodynamic Studies of Antigen-Antibody Interactions in Heterogeneous Reaction Phases-I. L-Thyroxin (T4) With Specific Antibody Immobilized on Controlled Pore Glass. Mol. Immunol. 1979; 16: 173-8.

4. Levison, S.A., Hicks, A.N., Portmann, A.J., Dandliker, W.B. Fluorescence Polarization and Intensity Kinetic Studies of Antifluorescein Antibody Obtained at Different Stages of the Immune Response. Biochemistry 1975; 14: 3778-86.

5. Finney, D.J., Response Curves for Radioimmunoassay. Clin. Chem. 1983; 29: 1762-6.

6. Rodbard, D. Statistical Quality Control and Routine Data Processing for Radioimmunoassays and Immunoradiometric Assays. Clin. Chem. 1974; 20: 1255-70.

7. Dudley, R.A., Edwards, P., Ekins, R.P., and Al. Guidelines for Immunoassay Data Processing. Clin. Chem. 1985; 31: 1264-71.

8. Rodbard, D., Feldman, Y. Kinetics of Two-Site Immunoradiometric (Sandwich) Assays-I. Immunochemistry 1978; 15: 71-6.

9. Hoffman, K.L., Parsons, G.H., Allerdt, L.J., Brooks, J.M., Miles, L.E. Elimination of "Hook-Effect" in Two-Site Immunoradiometric Assays by Kinetic Rate Analysis. Clin. Chem. 1984; 30: 1499-501.

10. Girolami, A., Sticchi, A., Melizzi, R., Saggin, L., Ruzza, G. Prothrombin Evaluation as Obtained by Kinetics Studies of Antigen-Antibody Reaction in a Laser Nephelometer. Thromb. Haemost. 1984; 52: 15-8.

11. Absolom, D.R. and van Oss, C.J. The Nature of the Antigen-Antibody Bond and the Factors Affecting its Association and Dissociation. CRC Crit. Rev. Immunol. 1986; 6: 1-46.

12. Mathis, G. Rare Earth Cryptates and Homogeneous Fluoro-immunoassays with Human Sera. Clin. Chem. 1993; 39: 1953-9.

13. Mathis, G., Socquet, F., Viguier, M., Darbouret, B., Jolu, E.J.P.J. Amplified Homogeneous Time-Resolved Immunofluorometric Assay of Prolactin [Abstract]. Clin. Chem. 1993; 39: 1251.

14. Lopez, E., Chypre, C., Alpha, B., Mathis, G. Europium(III) Trisbipyridine Cryptate Label for Time-Resolved Fluorescence Detection of Polymerase Chain Reaction Products Fixed on a Solid Support. Clin. Chem. 1993; 39: 196-201.

15. Wieder, I. Background Rejection in Fuorescent Immunoassay. In: Knapp, W., Hobular, K., Wick, G., ed. Immunofluorescence and Related Staining Techniques (Proceedings of VI International Conference on Immunofluorescence and Related Staining Techniques). Amsterdam: Elsevier Biomedical Press, 1978: 67-80.

16. Soini, E., Lövgren, T. Time Resolved Fluorescence of Lanthanide Probes and Applications in Biotechnology. Crit. Rev. Anal. Chem. 1987; 18: 105-54.

17. Mabile, M., Mathis, G., Jolu, E.J.P., Pouyat, D., Dumont, C. Method of Measuring Luminescence in an Assay by Luminescence. Patent WO 92/13264, 1991.

18. Lebreton, J.D., Millier, C. Modèles Dynamiques Déterministes en Biologie. Paris: Masson, 1982: 208pp.

19. Mason, R.L, Gunst, R.F., Hess, J.L. Statistical Design and Analysis of Experiments. New York: John Wiley & Sons, 1989: 692pp.

20. Beale, E.M.L. Confidence Regions in Non-Linear Estimation. J. R. Stat. Soc. 1960; 22B: 41-88.

21. Lobry, J.R., Rosso, L., Flandrois, J.P. A FORTRAN Subroutine for the Determination of Parameter Confidence Limits in Non-Linear Models. Binary 1991; 3: 86-93.

22. Rodbard, D., Munson, P.J., De Lean, A. Improved Curve-Fitting, Parallelism Testing, Characterization of Sensitivity and Specificity, Validation, and Optimization for Radioligand Assays. In: Radioimmunoassay and Related Procedures in Medicine 1977. Vienna: International Atomic Energy Agency, 1978: 469-504

23. Sadler, W.A., Smith, M.H. A Computer Program for Estimating Imprecision Characteristics of Immunoassays. Comput. Biomed. Res. 1988; 23: 105-14.

24. Seber, G.A.F., Wild, C.J. Non-Linear Regression. New-York: John Wiley & Sons, 1989: 768pp.

25. Tengerdy, R.P., Small, W.H. Reaction Kinetic Studies of the Antigen-Antibody Reaction. Nature 1966; 210: 708-10.